GmN70 and LjN70. Anion Transporters of the Symbiosome Membrane of Nodules with a Transport Preference for Nitrate[1]

Eric D. Vincill, Krzysztof Szczyglowski, and Daniel M. Roberts*

Department of Biochemistry and Cellular and Molecular Biology, The University of Tennessee, Knoxville, Tennessee 37996 (E.D.V., D.M.R.); and Agriculture and Agri-Food Canada, Southern Crop Protection and Food Research Centre, London, Ontario N5V 4T3, Canada (K.S.)

A cDNA was isolated from soybean (*Glycine max*) nodules that encodes a putative transporter (GmN70) of the major facilitator superfamily. GmN70 is expressed predominantly in mature nitrogen-fixing root nodules. By western-blot and immunocytochemical analyses, GmN70 was localized to the symbiosome membrane of infected root nodule cells, suggesting a transport role in symbiosis. To investigate its transport function, cRNA encoding GmN70 was expressed in *Xenopus laevis* oocytes, and two-electrode voltage clamp analysis was performed. Ooctyes expressing GmN70 showed outward currents that are carried by anions with a selectivity of nitrate > nitrite ≫ chloride. These currents showed little sensitivity to pH or the nature of the counter cation in the oocyte bath solution. One-half maximal currents were induced by nitrate concentrations between 1 to 3 mM. No apparent transport of organic anions was observed. Voltage clamp records of an ortholog of GmN70 from *Lotus japonicus* (LjN70; K. Szczyglowski, P. Kapranov, D. Hamburger, F.J. de Bruijn [1998] Plant Mol Biol 37: 651–661) also showed anion currents with a similar selectivity profile. Overall, these findings suggest that GmN70 and LjN70 are inorganic anion transporters of the symbiosome membrane with enhanced preference for nitrate. These transport activities may aid in regulation of ion and membrane potential homeostasis, possibly in response to external nitrate concentrations that are known to regulate the symbiosis.

During the formation of legume-rhizobia symbioses, the development of a specialized organ, the root nodule, is induced via the exchange of signals between the bacteria and plant host (Stougaard, 2000; Limpens and Bisseling, 2003). Ultimately, the bacteria infect a specialized plant cell (infected cell) within the core of the nodule and become enclosed in an organelle called the symbiosome, the major organelle of this cell type (Roth et al., 1988). This organelle is delimited by the plant-derived symbiosome membrane, which mediates the symbiotic exchange of nutrients (reduced carbon compounds from the plant cytosol in exchange for reduced nitrogen from the bacteroid), and serves to protect the endosymbiont from plant defense responses (for review, see Udvardi and Day, 1997; Day et al., 2001).

The biogenesis of the symbiosome membrane results in the acquisition of a number of transport activities that aid in the establishment and maintenance of the symbiosis. These include a dicarboxylate transport activity that facilitates the uptake of malate or succinate, which serve as carbon sources to support bacteroid nitrogen fixation (Ou Yang et al., 1990; Udvardi and Day, 1997), as well as transport pathways for the efflux of fixed nitrogen as NH_3 (Niemietz and Tyerman, 2000) or NH_4^+ (Tyerman et al., 1995; Day et al., 2001; Roberts and Tyerman, 2002). In addition, other transport activities have been documented on the mature symbiosome membrane including a proton pump that generates an electrogenic pH gradient that presumably drives metabolite exchange (Blumwald et al., 1985; Udvardi and Day, 1989), an aquaglyceroporin activity (Rivers et al., 1997; Dean et al., 1999) that may be involved in osmoregulation (Guenther et al., 2003), and transporters for iron and zinc uptake (Moreau et al., 2002; Kaiser et al., 2003).

Nodule development is associated with the spatially and temporally regulated expression of a number of nodule-enhanced transcripts (referred to as nodulins) that aid in the establishment of the symbiosis (for review, see Stougaard, 2000), including a number that encode membrane transport proteins (Fortin et al., 1987; Szczyglowski et al., 1998; Moreau et al., 2002; Kaiser et al., 2003; Jeong et al., 2004) and proteins associated specifically with the symbiosome membrane (Fortin et al., 1985; Panter et al., 2000; Saalbach et al., 2002; Wienkoop and Saalbach, 2003; Catalano et al., 2004). Analysis of expressed sequence tags (ESTs) obtained during nodule organogenesis of the model legume *Lotus japonicus* revealed a late-nodulin *LjN70* that encodes a polytopic membrane protein with a topology and sequence similarity to members of the major facilitator superfamily (MFS) of membrane

[1] This work was supported by the National Science Foundation (grant no. MCB–0237219 to D.M.R.).

* Corresponding author; e-mail drobert2@utk.edu; fax 865–974–6306.

Article, publication date, and citation information can be found at www.plantphysiol.org/cgi/doi/10.1104/pp.104.051953.

transporters (Szczyglowski et al., 1998). In this study, we have isolated an ortholog of this protein (GmN70) from soybean (*Glycine max*) and show that it is a symbiosome membrane protein that possesses an anion transport activity with a selectivity for nitrate, nitrite, and chloride.

RESULTS

Isolation of a Full-Length cDNA Encoding GmNod70LP

A set of primers for reverse transcription (RT)-PCR were designed based on conserved sequences from LjN70 (Szczyglowski et al., 1998) and LjN70-like proteins from Arabidopsis (*Arabidopsis thaliana*). RT-PCR of mRNA from mature (28-d) soybean nodules amplified a 1,269-bp product with high sequence similarity to LjN70. A full-length sequence was deduced from 5′-RACE of nodule cDNA and from the analysis of the 3′-regions of partial EST sequence libraries from soybean. This sequence was confirmed by RT-PCR amplification of a full-length cDNA from soybean nodule mRNA (Fig. 1). The resulting open reading frame (ORF; 598 amino acids) shows considerable amino acid sequence similarity (52% identity) to LjN70. Similar to LjN70, hydropathy analysis predicts a topology with 12 putative transmembrane regions (Fig. 1) separated by a large extended hydrophilic loop between helices 6 and 7, similar to members of the MFS (Pao et al., 1998).

Northern-blot analysis of total RNA from various tissues of 28-d-old soybean plants shows high expression of this transcript in nodule tissue, with lower amounts of signal detected in leaf and root tissues (Fig. 2A). Because of its similarity to LjN70 and high expression in nodules, the protein encoded by this cDNA is referred to as *Glycine max* N70-like protein (GmN70).

Preparation of a Site-Specific Antibody against GmNod70-LP and Immunolocalization

A unique hydrophilic region within the putative central loop of GmN70 was chosen to prepare a synthetic peptide antigen (CD-18) for antibody production (Fig. 1). Western-blot analysis of nodule membrane extracts shows that the anti-CD-18 antibody cross reacts with a protein with an apparent molecular mass of 68 kD (Fig. 2B), similar to the proposed molecular mass of GmN70 based on its deduced amino acid sequence.

To determine the localization and expression pattern of the GmN70 gene product in soybean nodule tissue, immunocytochemistry was performed with affinity-purified anti-CD-18 antibodies (Fig. 3). Epifluorescent images of nodule tissue showed high levels of GmN70 immunoreactivity in the central infection zone and not in the inner and outer cortical regions of the nodule (Fig. 3C), similar to soybean nodulin 26 (Fig. 3E), a well-characterized nodule-specific membrane protein that is specifically expressed at a high concentration on the symbiosome membrane in infected cells (Fortin et al., 1987; Weaver et al., 1991). At higher magnifications of the central infection zone, detection of GmN70 was limited to infected cells with no signal detected above background in adjacent uninfected cells (Fig. 3D). No signal was detected in control samples probed with preimmune sera (Fig. 3G).

Since immunocytochemical evidence suggests a specific expression pattern of GmN70 in infected cells, the possibility that this protein is localized to the symbiosome membrane was pursued. Immunoblot of isolated, purified symbiosome membranes showed the presence of an immunoreactive band at 68 kD, suggesting that GmN70 is found on the symbiosome membrane (Fig. 2).

Analysis of GmN70 by Two-Electrode Voltage Clamp of Xenopus Ooctyes

To investigate the transport properties of GmN70, cRNA was prepared by in vitro transcription and was microinjected into Xenopus ooctyes. After 3 d of culture, western-blot analysis indicated the expression of GmN70 in oocytes (data not shown). Transfer of these oocytes from Frog Ringer's solution into an identical bath solution in which NaCl was replaced by sodium-gluconate resulted in a depolarization of the resting membrane potential (from −16 mV to −3.7 mV; Table I). Subsequent perfusion with an identical buffer in which gluconate was replaced with nitrate resulted in a hyperpolarization of the oocyte membrane (V_m = −27 mV). Analysis of the membrane currents of the GmN70 oocytes by two-electrode voltage clamp recording showed that nitrate also induced elevated outward steady-state currents (Fig. 4A) and shifted the reversal potential of the oocyte to a more negative value (Table I). In contrast, uninjected control oocytes showed little change in resting V_m (Table I) or in membrane currents (Fig. 4C) in response to these various anions in the recording bath. The data suggest that GmN70 mediates the uptake of nitrate by the oocyte.

Analysis of the currents induced by various concentrations of nitrate in the recording bath showed that increasing the concentration of NO_3^- resulted in an increase in outward current and a corresponding shift in oocyte reversal potential to more negative values consistent with the increase in the equilibrium potential of nitrate (Fig. 5). Plots of the intensity of this outward current versus nitrate concentration show an I_{max} with a linear dependence on V_m and a $K_{0.5}$ value ($[NO_3^-]$ that induces one-half maximal current) ranging from 1 mM (+75 mV) to 3 mM (+15 mV; Fig. 5C).

Since many members of the MFS exhibit cotransport of protons or other cations as part of their mechanism of transport (Pao et al., 1998), the dependence of nitrate transport on pH and the nature of the counter cations

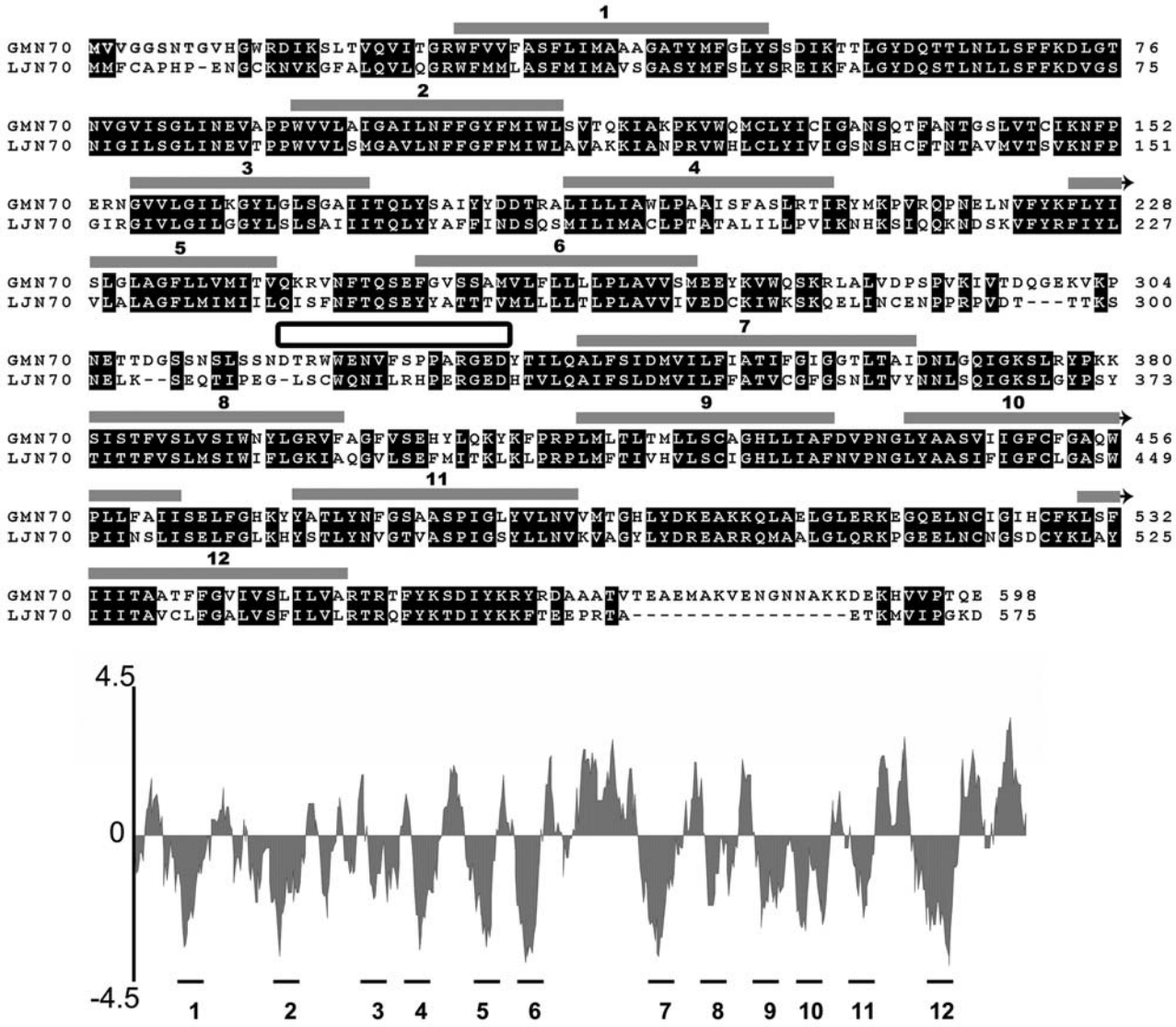

Figure 1. Comparison of the deduced amino acid sequences of GmN70 and LjN70. Regions of high sequence conservation are boxed in black. Regions proposed to form transmembrane α-helices (represented by gray-shaded boxes above the sequence) were identified from a hydropathy plot (shown below the aligned sequences) by using the Kyte-Doolittle algorithm (Kyte and Doolittle, 1982) in the DNAstar software package. The sequence that was used to make a synthetic peptide antigen for site-specific antibody formation is indicated by the box between α-helices 6 and 7.

was investigated (Fig. 6). The magnitude of the nitrate currents generated at pH 5 was indistinguishable from those at pH 7.6 and showed no difference in response to Na^+, K^+, or the impermeable *N*-methyl-D-glucamine, suggesting that the nature of the counter cation has little effect on GmN70-mediated transport.

To investigate the selectivity of transport, currents induced by a series of anions in the bath solution were analyzed (Fig. 7). Oocytes bathed in nitrate and nitrite yielded outward currents of similar intensity. Substitution of chloride generated currents of diminished intensity, whereas currents generated with organic anions (acetate, malate, and succinate) showed little difference from the negative control anion gluconate. In addition to differences in the current magnitude, chloride currents showed more positive reversal potentials than those induced by an equivalent concentration of nitrate (Table I). Based on the difference of these reversal potentials, a permeability ratio ($P_{\text{nitrate}}/P_{\text{Cl}-}$) of 2.23 (SEM = 0.21; $n = 7$) was determined for oocytes expressing GmN70.

Voltage clamp recording of oocytes expressing the orthologous protein LjN70 (Szczyglowski et al., 1998) also show outward currents in the presence of nitrate and nitrite but exhibited little apparent permeability to chloride or organic anions. Overall, the data suggest that GmN70 and LjN70 are nodule anion transport proteins with a selectivity preference for nitrate.

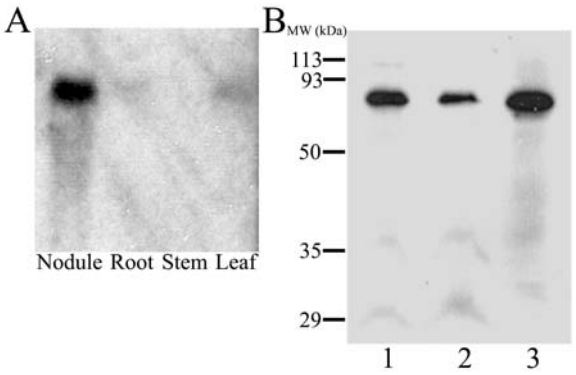

Figure 2. Northern- and western-blot analyses of GmN70. A, Total RNA samples (40 μg/lane) from nodule, root, stem, and leaf tissues of 28-d-old soybean were resolved by electrophoresis on a 1.2% (w/v) agarose-formaldahyde denaturing gel, and GmN70 mRNA was detected by northern-blot analysis as described in ''Materials and Methods.'' B, Purified symbiosome membranes (lanes 1 and 2) and a nodule microsomal fraction (lane 3) were resolved by SDS-PAGE on a 12.5% (w/v) polyacrylamide gel. Each lane contains 15 μg of protein. The resolved proteins were analyzed by western-blot analysis with affinity-purified anti-CD-18 antibodies as described in ''Materials and Methods.''

DISCUSSION

GmN70 represents an ortholog of the nodulin LjN70, a protein expressed during the late developmental stages of *L. japonicus* nodule organogenesis (Szczyglowski et al., 1998). Similar to LjN70, GmN70 mRNA shows enhanced expression in mature nodules. By immunolocalization and western-blot analyses, GmN70 shows preferential expression on the symbiosome membrane within infected cells of soybean nodules. Both LjN70 and GmN70 appear to encode a polytopic membrane protein with 12 putative transmembrane regions organized in 2 groups of 6 with a large hydrophilic-loop region between, a topology similar to MFS transporters (Pao et al., 1998). The MFS is a diverse family found in all prokaryotes and eukaryotes, and represents a large collection of membrane transporters of a wide range of substrates including sugars, drugs, organic and inorganic ions, Krebs-cycle intermediates, amino acids, and peptides (Pao et al., 1998).

Xenopus oocytes expressing GmN70 displayed distinct electrophysiological properties. Perfusion of these oocytes with a solution in which chloride was replaced by the impermeant anion gluconate resulted in depolarization of the plasma membrane. Subsequent perfusion with solutions containing chloride or nitrate resulted in restoration of negative membrane potentials and the induction of outward currents measured by two-electrode voltage clamp recording. It has been noted that Xenopus oocytes have an endogenous calcium-induced voltage-activated chloride channel (Dascal, 1987; Machaca and Hartzell, 1999). The measured currents in GmN70 oocytes are distinguished from these endogenous currents since (1) they show no time-dependent openings or desensitization, (2) replacement of Ca^{2+} ions in the bath with Mg^{2+} or Mn^{2+} does not affect the currents (data not shown), and (3) uninjected control oocytes do not show any of the behaviors listed above for the GmN70 oocytes. Collectively, these results suggest that GmN70 is permeable to both chloride and nitrate. Further, the permeability to chloride explains the depolarization observed upon perfusion of oocytes with gluconate and suggests that either inward or outward transport are possible through GmN70. Based on the magnitude of the current and differences in the reversal potential from I/V plots, nitrate is favored over chloride as a transport substrate.

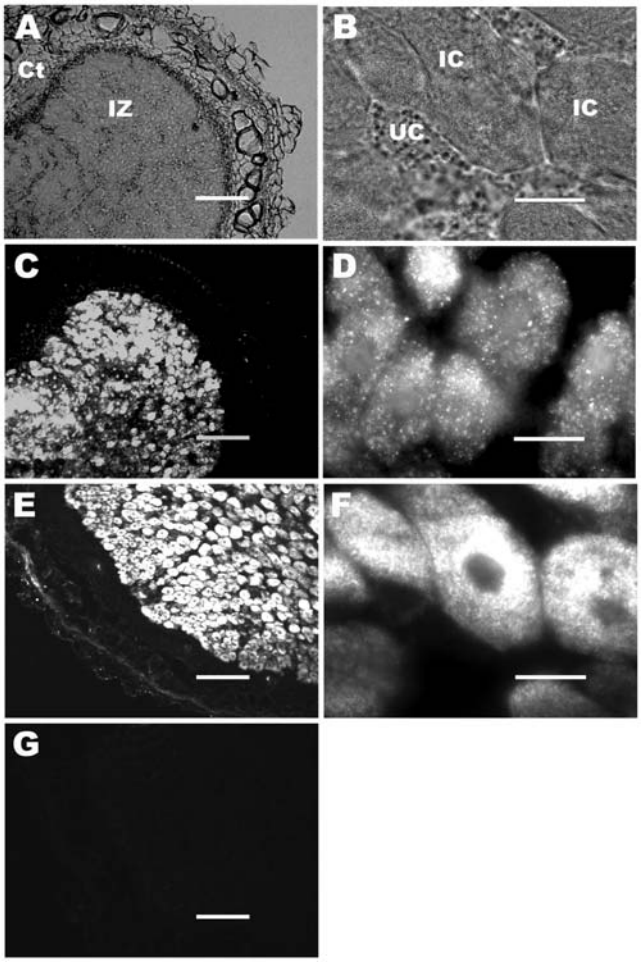

Figure 3. Immunolocalization of GmN70 in soybean nodules. Nodule sections from 28-d-old soybeans were fixed, sectioned, and immunostained as described in ''Materials and Methods.'' A, Nodule section viewed by phase contrast light microscopy at low magnification with the infection (IZ) and cortical cell (Ct) zones indicated. B, A higher magnification micrograph of A, showing infected cells (IC) and uninfected companion cells (UC) of the infection zone. C and D, Nodule section probed with affinity-purified anti-GmN70 antibody. E and F, Nodule section probed with anti-nodulin-26 antibody (infected cell/symbiosome membrane control). G, Nodule section probed with preimmunization sera. The bars for A, C, E, and G are 150 μm. The bars for B, D, and F are 20 μm.

Table I. *Resting membrane potentials and reversal potentials of GmN70 oocytes in the presence of gluconate or nitrate*

Oocyte[a]	Resting Membrane Potential			Reversal Potentials[c]		
	Gluconate[b]	Nitrate	Chloride	Gluconate	Nitrate	Chloride
Uninjected	−33.8 mV (2.9; n = 11)[d]	−33.5 mV (1.5; n = 11)	−26.5 mV (3.4; n = 21)	−32.1 mV (5.0; n = 8)	−31.6 mV (2.8; n = 8)	−26.7 mV (3.4; n = 8)
GmN70 injected	−3.8 mV (1.2; n = 26)	−27.8 mV (1.0; n = 26)	−16.0 mV (0.6; n = 28)	−5.1 mV (1.3; n = 22)	−27.3 mV (1.1; n = 22)	−13.2 mV (2.6; n = 10)

[a]Oocytes were injected with 45 ng of the indicated cRNA and were cultured for 3 to 4 d in Frog Ringer's solution as described in "Materials and Methods." [b]Bath solutions consisted of 10 mM HEPES-NaOH, pH 7.6, 6 mM $CaCl_2$, 2 mM $MgCl_2$, and 100 mM of the sodium salt of the indicated anion. [c]Reversal potentials were calculated from *I-V* plots of recordings similar to those in Figure 4A. [d]Numbers in parentheses represent SEM.

Functional analysis of plant nitrate transporters of the MFS family shows that they are members of one of two families, the nitrate-nitrite transport family, which encode high-affinity nitrate transporters (NRT2 family) and a lower affinity nitrate transporter family (NRT1 family) with sequence similarity to the peptide transporters of yeast and plants (for review, see Forde, 2000; Orsel et al., 2002). Based on the measured $K_{0.5}$ of nitrate transport by GmN70 (1–3 mM), it would be classified as a lower affinity transporter. However, unlike both NRT1 and 2 transporters, GmN70 shows no apparent dependence on protons or cations for transport, and has a sequence that is distinct from both classes of nitrate transporters. Indeed, a comparison of GmN70 and LjN70 with MFS family members for which a function is documented shows that they are divergent in sequence with only a slight similarity with the *Oxalobacter formigenes* oxalate:formate exchange protein (OxlT; 30% similarity; Abe et al., 1996; Szczyglowski et al., 1998) and the murine monocarboxylate transporter 1 (MCT-1; 34% similarity; Carpenter et al., 1996). Similar to GmN70, OxlT and MCT-1 exhibit a substrate specificity for anions (Abe et al., 1996; Carpenter et al., 1996).

However, examination of the genomes and EST libraries reveals that a subfamily of proteins with a higher degree of similarity to GmN70 and LjN70 is present in a variety of plant species (Fig. 8). An

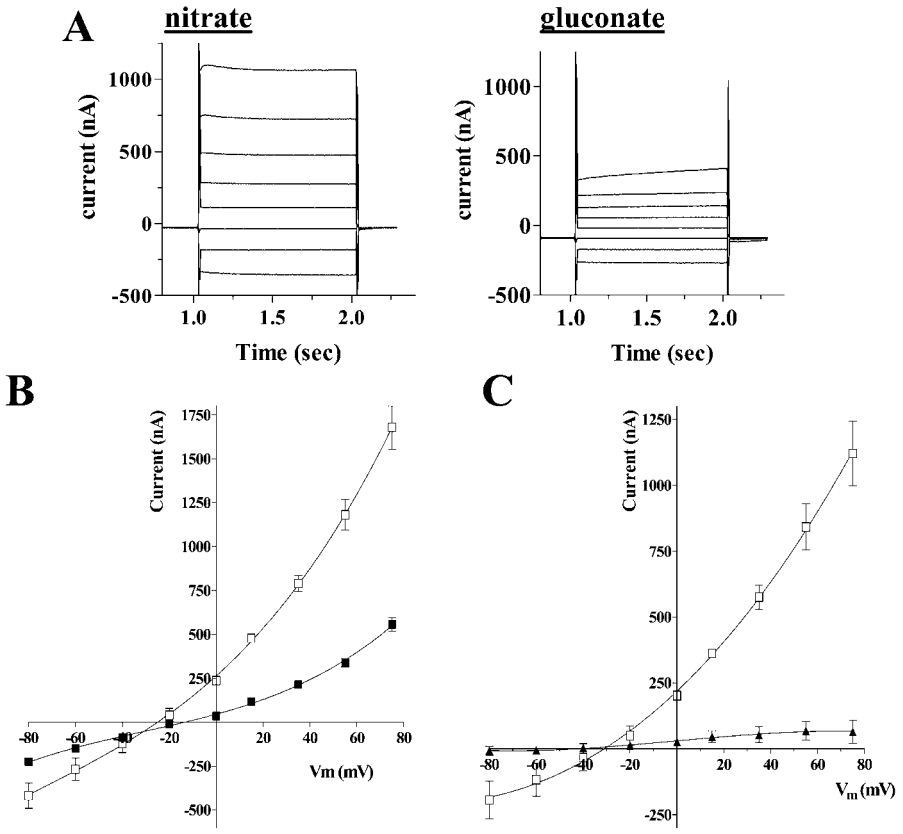

Figure 4. Nitrate-induced currents in Xenopus oocytes expressing GmN70. Oocytes were injected with GmN70 cRNA and were cultured for 4 d prior to two-electrode voltage clamp recording as described in "Materials and Methods." A, Current records from a GmN70-injected oocyte bathed in 100 mM $NaNO_3$ or 100 mM sodium gluconate in the presence of standard recording-bath solution. The plot represents the currents obtained from a step-wise voltage protocol in which oocytes were recorded at V_m clamped from +60 to −80 mV in 20-mV increments. Each potential was maintained for 1 s with a 0.5-s recovery period at a holding potential of −35 mV between each voltage pulse. B, Plot of steady-state currents versus clamped membrane potential (V_m) of GmN70 oocytes bathed in 100 mM Na NO_3 (white squares) or 100 mM Na gluconate (black squares). Error bars show SEM of currents recorded from three separate oocytes. C, Current voltage relationship of nitrate-induced currents corrected for background currents (in the presence of gluconate) for GmN70-injected oocytes (white squares) or uninjected control ooctyes (black triangles).

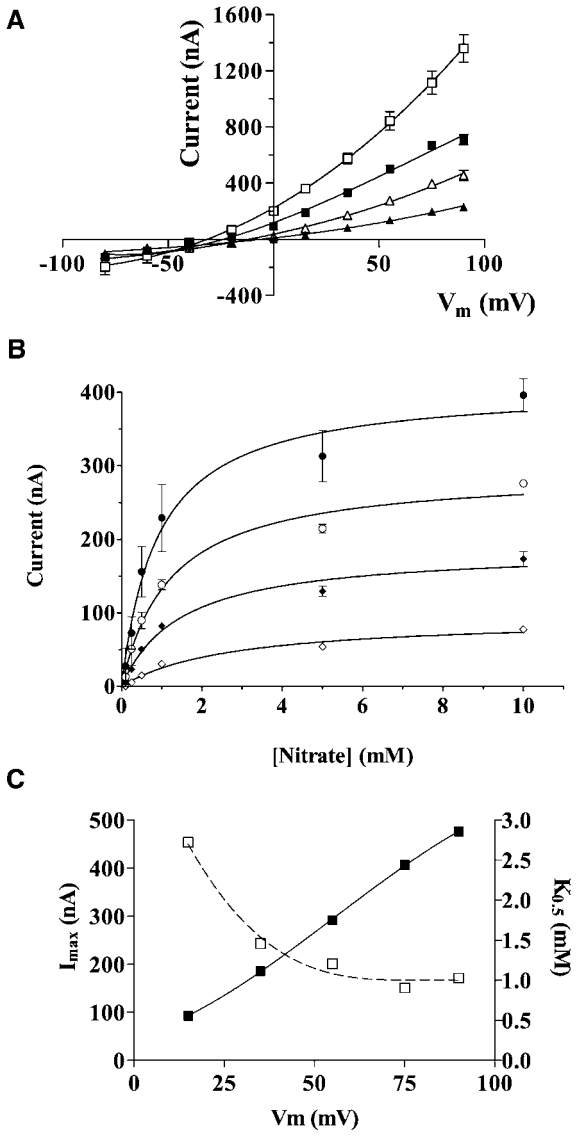

Figure 5. Concentration dependence of nitrate-induced currents in Xenopus oocytes expressing GmN70. Oocytes expressing GmN70 were analyzed by voltage clamp recording under standard conditions in the presence of varying concentrations of sodium nitrate in the bath. A, *I-V* plots of oocytes in the presence of 100 mM (white squares), 25 mM (black squares), 10 mM (white triangles), and 1 mM (black triangles) sodium nitrate. B, Plot of steady-state currents as a function of bath nitrate concentration recorded at V_m values of +75 mV (black circles), +55 mV (white circles), +35 mV (black diamonds), and +15 mV (white diamonds). Data are the average of determinations from three oocytes with error bars showing the SEM. C, I_{max} (black squares) and $K_{0.5}$ values (white squares) for nitrate-induced outward oocyte currents are expressed as a function of membrane potential (V_m).

inspection of the annotated Arabidopsis genome revealed 2 genes (At2g39210 and At2g28120) that encode proteins with 65% and 57% sequence identity to GmN70, respectively. Preliminary transport analyses of the Arabidopsis gene products by expression in Xenopus oocytes suggest that they exhibit transport properties similar to LjN70 and GmN70 (data not shown). This finding suggests that plants contain a subfamily of closely related anion/nitrate transporters related to GmN70 that may have a broader role beyond symbiosis. This is supported by examination of the soybean EST libraries, which shows that GmN70 is among several closely related cDNAs (ranging from 57%–87% identity to GmN70), some of which are expressed in other organs besides the nodule. Whether these are responsible for some of the anion/nitrate transport activities documented on other plant membranes remains to be determined. Since these plant proteins appear to represent a structurally and functionally related family of anion transporters, we suggest a name for this family of "nodulin-like anion transport proteins" (NLAT; Fig. 8).

The transport properties of the symbiosome membrane have attracted considerable interest given the pivotal role that this plant-derived membrane plays in nitrogen-fixing symbioses (Udvardi and Day, 1997; Day et al., 2001). The membrane is energized by an ATPase pump that generates an electrical and pH gradient by transporting protons into the lumen of the

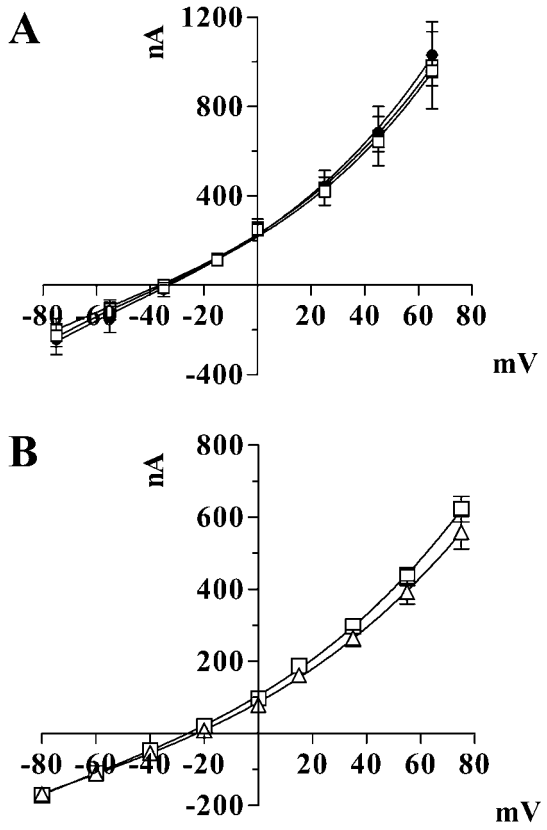

Figure 6. GmN70 currents are independent of cations and pH. A, GmN70-injected oocytes were subjected to voltage clamp recording in 100 mM NO_3^- salts of the following cations: Na^+ (white squares), K^+ (black circles), and *N*-methyl-D-glucamine (white circles). B, Recordings of GmN70-injected oocytes in the presence of 100 mM sodium nitrate at pH 7.6 (white squares) and pH 5.0 (white triangles). The data are the average of recordings from three oocytes with error bars showing the SEM.

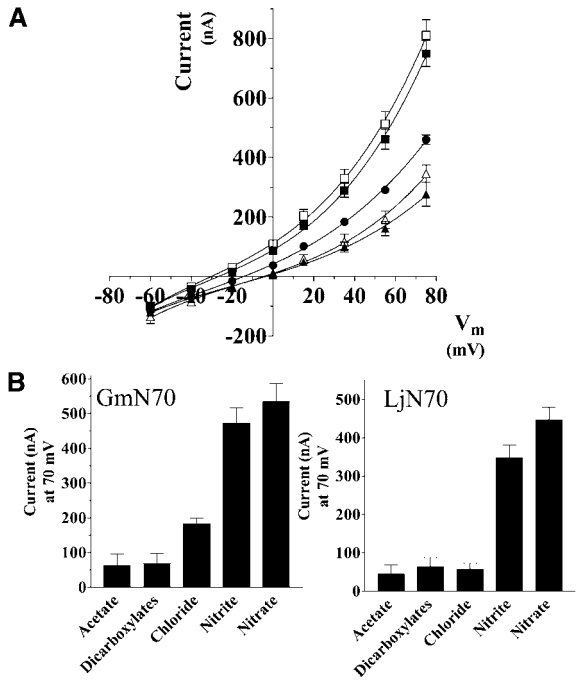

Figure 7. Anion selectivity of GmN70 and the *L. japonicus* ortholog LjN70. A, Oocytes injected with GmN70 cRNA or LjN70 cRNA were subjected to voltage clamp under standard conditions. A, GmN70-injected oocyte *I-V* plots in the presence of 100 mM $NaNO_3$ (white squares), 100 mM $NaNO_2$ (black squares), 100 mM NaCl (black circles), 66 mM sodium dicarboxylates (33 mM malate and 33 mM succinate, white triangles), and 100 mM sodium acetate (black triangles). B, Steady-state currents for GmN70 or LjN70-injected oocytes at +75 mV obtained with each of the indicated anions. The currents shown in the histograms were corrected for background currents by subtraction of basal currents obtained with gluconate substituted as the test anion. The error bars showing the SEM (n = 3 oocytes).

symbiosome (Udvardi and Day, 1989). This gradient has been proposed to play an important role in driving the uptake of dicarboxylates as an energy source to support nitrogen fixation by the bacteroid (Ou Yang et al., 1990) and also is proposed to regulate the release of fixed NH_4^+ through an inwardly rectified voltage-dependent cation channel (Tyerman et al., 1995; Roberts and Tyerman, 2002). Additionally, the pH of the lumen is thought to be an important factor controlling pH-sensitive hydrolytic activities within the symbiosome, which is considered to be a lytic organelle (Brewin, 1991). By using the potential-sensitive dye oxonol V, it was previously shown that the $\Delta\Psi$ generated by the H^+-ATPase in isolated intact soybean symbiosomes can be collapsed by the addition of anion salts, suggesting an anion transporter on the symbiosome membrane (Udvardi and Day, 1989; Udvardi et al., 1991). Interestingly, the effectiveness of the various anion salts to dissipate the soybean symbiosome membrane $\Delta\Psi$ is similar to the permeability profile of the GmN70 that we report here (nitrate > nitrite $\gg$ chloride $\ggg$ acetate = dicarboxylates). The finding of GmN70 on symbiosome membranes supports the hypothesis that this protein is responsible for this activity measured with isolated symbiosomes.

What potential function would an anion/nitrate transporter play on the symbiosome membrane? While the functional significance of this activity is unclear, several potential roles are possible. First, the $\Delta\Psi$ generated by the H^+-ATPase on the symbiosome membrane drives the transport of permeate anions into the symbiosome space resulting in a conversion of the $\Delta\Psi$ to a ΔpH. Indeed, it has been observed that isolated soybean symbiosomes undergo a slow acidification in the presence of chloride or nitrate anions in response to the addition of ATP (Udvardi et al., 1991). Coordinate regulation of these transport processes would control the transmembrane potential of the symbiosome membrane as well as the pH of the symbiosome space. Additionally, since the symbiosome is the major intracellular organelle of the infected cell, anion transport may also play a role in osmoregulation and cytosolic ion homeostasis, similar to the function that has been proposed for anion transport on the tonoplast membrane of vacuoles of other plant cell types (Barbier-Brygoo et al., 2000).

The selectivity for nitrate is also interesting in light of the fact that nitrogen-fixing symbioses are induced under nitrogen-poor conditions (i.e. low-soil nitrate). Indeed, in the presence of nitrate (a preferred source of nitrogen), nodule development is suppressed, nitrogen fixation of existing nodules is inhibited, and senescence is promoted (Streeter, 1988; Carroll and Mathews, 1990). The effects of nitrate on these

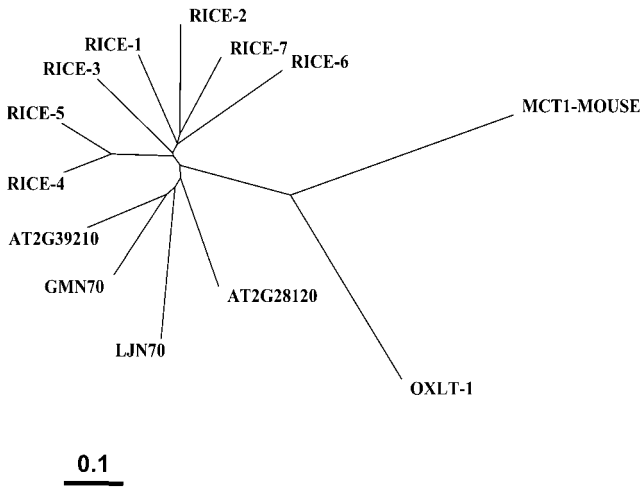

Figure 8. Phylogenetic analysis of GmN70-like anion transporter family with MCT-1 and OxlT-1. Shown is a phylogenetic tree of the full-length deduced amino acid sequences of the following N70-like proteins: Rice N70-like ESTs (Rice-1–7 respective accession nos.: TC235634, TC238235, NP937656, NP889385, TC217196, TC244401, TC222019); the 2 Arabidopsis N70-like proteins (accession nos. At2g39210-AAL31925, At2g28120-AAL14413); and GmN70 and LjN70. The relationship to mouse MCT-1 and *O. formigenes* OxlT-1 proteins (National Center for Biotechnology Information accession nos. LjN70-AAC3950, OxlT1-Q51330, MCT1-P53986) are shown. Scale bar = 0.1 amino acid substitutions/site.

processes is complex and involves a variety of temporally controlled physiological changes including restriction of oxygen diffusion into the infected zone (Carroll et al., 1987), deprivation of carbohydrate supply to the nodule (Streeter, 1988), and production of reactive oxygen species (Matamoros et al., 1999). It has been suggested previously (Udvardi and Day, 1989) that nitrate uptake via an anion transporter on the symbiosome membrane could uncouple the H^+-ATPase pump in response to elevated cytosolic nitrate levels. This in turn could result in a reduction of the symbiosome membrane potential and a reduced driving force for the symbiotic uptake of dicarboxylates (Ou Yang et al., 1990) and the efflux of fixed ammonium ion (Tyerman et al., 1995). Alternatively, nitrate uptake by symbiosomes may directly affect bacteroid metabolism since increases in soil nitrate induce enhanced levels of bacteroid nitrate and nitrite reductases and a concomitant decrease in nitrogenase activity (Arrese-Igor et al., 1997; Luciński et al., 2002). These could provide an additional control of nitrogen fixation in response to the availability of alternative nitrogen sources.

MATERIALS AND METHODS

Nucleic Acid and Molecular Cloning Techniques

Nodulated soybean (*Glycine max*) cv Essex plants infected with *Bradyrhizobium japonicum* strain USDA 110 were grown as previously described (Weaver et al., 1991). Total RNA was isolated from 28-d-old nodules by guanidinium thiocyanate extraction and differential LiCl precipitation as described in Guenther and Roberts (2000). cDNA was generated from nodule RNA preparations by RT using the SuperScript First-Strand Synthesis System (Invitrogen, Carlsbad, CA). A partial cDNA clone was generated by touchdown PCR (parameters: denaturation 94°C, 1 min; annealing [65°C to 57°C at 2-degree increments every third cycle and then 15 cycles at 48°C], 30 s; extension 72°C, 2 min) with the following primer set: F-5′-TATGACCAATCCACTCTCAAT, R-5′-GTATGACCCAATTGGACTTGC.

The cDNA fragment encoding part of the GmN70 ORF was cloned into the TOPO-TA vector following the manufacturer's protocol (Invitrogen). Upstream 5′ regions of the ORF were obtained by using total nodule cDNA and 5′ RACE (TakaRa Biomedicals, Madison, WI). The 3′ end was identified from analysis of a soybean EST library (accession no. TC142224; www.tigr.org). From these sequences, a contiguous cDNA containing the full ORF was obtained by PCR of nodulin cDNA using the following primer set: F-5′-ATGGTAGTTGGAGGTTCGAATACC, R-5′-TTACTTCTGAGTTGGCATCACATG.

*Bgl*II restriction sites were engineered into the 5′ end of the primers to facilitate cloning into the pXβG-ev1 expression vector (Preston et al., 1992) for functional expression in *Xenopus laevis* ooctyes (discussed below).

Automated DNA sequencing of both strands of all constructs was performed on a Perkin-Elmer Applied Biosystems (Foster City, CA) 373 DNA sequencer at the University of Tennessee Molecular Biology Research Facility (Knoxville, TN) using M13 reverse and forward primer sites. Sequence alignments were done by using ClustalW multiple sequence alignment program (version 1.7, June 1997) and the Blosum62 algorithm (Seqtools software package, www.seqtools.dk). Phylogenetic trees were constructed using the TreeView program of the same software package. The DNA and protein sequence information for GmN70 has been deposited (GenBank accession no. AY726670).

For northern-blot analysis, total RNA (40 μg) was resolved by electrophoresis on 1.2% (w/v) agarose gels in the presence of 5.6% (w/v) formaldehyde (Sambrook et al., 1989). RNA was blotted onto Zeta-Probe nylon membranes (Bio-Rad, Hercules, CA) and was prepared for northern-blot hybridization as described previously (Guenther and Roberts, 2000). Blots were hybridized with 10^6 cpm/mL of the GmN70 cDNA labeled with (α-^{32}P)dATP by nick translation (Promega, Madison, WI). The membranes were washed twice at 65°C in 1 mM EDTA, 40 mM $NaPO_4$, pH 7.2, 5% (w/v) SDS for 30 min and were exposed to x-ray film at −80°C for 7 d.

Immunochemical Techniques

Peptide antigens corresponding to the large central loop region of GmN70 (CD-18 peptide with the sequence CDTRWWENVFSPPARGED) or nodulin 26 (C-loop peptide with the sequence CMGNHDQFSGTVPNGT) were prepared synthetically (Invitrogen). Peptides were coupled to maleimide-activated keyhole limpet hemocyanin (Pierce-Endogen Chemicals, Rockford, IL) through amino-terminal Cys residues as described previously (Guenther et al., 2003). The resultant peptide-keyhole limpet hemocyanin conjugate was used to immunize New Zealand white rabbits (Weaver et al., 1991). Antisera were collected and antibodies were affinity purified as described in Guenther et al. (2003).

Western immunoblots of proteins resolved by SDS-polyacrylamide electrophoresis were done as described in Weaver et al. (1991) and Zhang and Roberts (1995), and immunoreactivity was assayed by chemiluminescent detection (Guenther et al., 2003). Symbiosome membranes were isolated from the nodules of 28-d soybean plants essentially as described in Rivers et al. (1997).

For immunolocalization, soybean nodules were cut into 1- to 2-mm slices with a razor blade and were immersed in 4% (w/v) paraformaldehyde in phosphate-buffered saline (PBS; 137 mM NaCl, 2.7 mM KCl, 9.6 mM NaH_2PO_4, 1.5 mM K_2HPO_4, pH 7.3) at 4°C for 16 h. Tissue samples were washed twice in PBS for 1 h and then were cryoprotected in 20% (w/v) Suc for 20 h at 4°C. Samples were then transferred to optimal cutting temperature compound (OCT; Fisher Scientific, Suwanee, GA) for 6 h at room temperature. The samples were then placed in embedding moulds with fresh OCT compound, were flash frozen in liquid nitrogen, and were stored at −80°C.

Embedded tissue blocks were equilibrated at −20°C for 4 h, and 6-micron sections were cut on a vibratome cryostat (Fisher Scientific), transferred to poly-L-lysine-coated coverslips, and stored at −20°C. For immunostaining, sections were washed in PBS to remove OCT compound and were incubated in blocking buffer (5% [v/v] normal goat serum, 2% [w/v] bovine serum albumin, 0.05% [w/v] Triton X-100 in PBS) for 45 min at room temperature. The sections were then incubated with antibodies or preimmunization sera controls in blocking buffer at 37°C for 2 h. The sections were washed 3 times in PBS at room temperature and were then incubated at 37°C for 1 h in Alexa 647-conjugated goat anti-rabbit IgG (Molecular Probes, Eugene, OR) diluted 1:100 in blocking buffer. The stained sections were washed three times in PBS and were mounted in anti-fade (Molecular Probes). Staining was visualized with an Axioplan microscope (Zeiss, Jena, Germany) equipped with an HBO 100-W mercury lamp for epifluorescence and with a scientific-grade cooled charge-coupled device. Visualization was done using a far-red (685 nm) filter. Grayscale digital images were collected, pseudocolored, and merged using the Metamorph Software (Universal Imaging, West Chester, PA).

Electrophysiological Techniques

The GmN70 insert was subcloned into the *Bgl* II site of pXβG-ev1 plasmid downstream of the T3 promoter. Full-length LjN70 (Szczyglowski et al., 1998) was cloned into the *Bgl*II and *Spe*I sites of the Xenopus expression vector pT7TS (Krieg and Melton, 1984). Capped cRNA was synthesized by in vitro transcription by using the mMESSAGE mMACHINE kit (Ambion, Austin, TX) essentially as in Guenther and Roberts (2000). Xenopus oocytes (stages V and VI) were surgically harvested as previously described (Guenther and Roberts, 2000) and were injected with 46 nL of cRNA (0.75 μg/μL). Microinjected oocytes or uninjected controls were cultured in Frog Ringer's solution (96 mM NaCl, 2 mM KCl, 5 mM $MgCl_2$, 0.6 mM $CaCl_2$, 5 mM HEPES-NaOH, pH 7.6) supplemented with 1,000 units/mL penicillin-streptomycin at 18°C for 3 to 4 d prior to analysis by two-electrode voltage clamp. Expression of GmN70LP or LjN70 in oocytes was verified by western blot with corresponding antibodies to each.

Oocyte recordings were done by two-electrode voltage clamp by using an Oocyte Clamp Amplifier model OC-725C (Warner Instruments, Hamden, CT). The microelectrodes were filled with 3 M KCl and tipped with 2% agarose-3M KCl to reduce KCl leakage (electrode resistances < 1.5 MΩ). The standard recording bath solution consisted of 2 mM KCl, 5 mM $MgCl_2$, 6 mM $CaCl_2$, 5 mM HEPES-NaOH, pH 7.6, containing 100 mM of the sodium salt of the test anion

conductant (final solution osmolarity = 215 mosm/kg). Recordings were performed using a step-wise voltage protocol in which the oocyte V_m was clamped from +80 to −80 mV in 20-mV increments. Each potential was maintained for 1 s with a 0.5-s recovery period at a holding potential of −35 mV between each voltage pulse. Voltage pulses were controlled with the Labscribe program suite version 1.6 (iWork; CB Sciences, Dover, NH). Membrane current (I_m) output was filtered at 1 kHz with a 4-pole Bessel Filter, was digitized via the iWork/118 analog to digital converter hardware, and was analyzed using the Labscribe software. Current convention was such that outward current refers to the movement of cations toward the bath and anions into the oocyte.

In experiments testing nitrate conductance at pH 5.0, 5 mM HEPES was replaced with 5 mM MES. In experiments in which the concentration of nitrate was varied, the osmolarity was adjusted to that of the standard buffer by using sodium gluconate. Steady-state membrane currents (I) were fit to the following equation:

$$I = \frac{I_{max}[NO_3^-]}{K_{0.5} + [NO_3^-]},$$

where I is steady-state current measured at +75 mV, I_{max} is the maximal current, and $K_{0.5}$ is the concentration of bath NO_3^- that induces one-half I_{max}.

Permeability comparisons for the various anions were done by substitution of the test anion for gluconate in the bath and evaluation of the induced currents. The permeability ratio P_{NO3}/P_{Cl} was determined by the difference in reversal potentials between recordings of identical oocytes under two bath conditions with differing anion concentrations: condition 1 contained 100 mM NO_3^- and 16 mM Cl^-, and condition 2 contained 116 mM Cl^-. The concentrations of cations and buffer salts were identical for both conditions. It was assumed that the internal oocyte Cl^- concentration is 33 mM and that the internal nitrate concentration is negligible (Dascal, 1987). From these assumptions, the following form of the Goldman-Hodgkin-Katz voltage equation was used:

$$\Delta E_{rev} = -\frac{RT}{F}\ln\frac{[Cl]_{out1} + P_{NO3}/P_{Cl}[NO_3]_{out1}}{[Cl]_{out2}},$$

where ΔE_{rev} is the difference in reversal potential between condition 1 and condition 2, R is the gas constant, T is the absolute temperature, and F is Faraday's constant.

Sequence data from this article have been deposited with the EMBL/GenBank data libraries under accession numbers AY726670, TC235634, TC238235, NP937656, NP889385, TC217196, TC244401, TC222019, At2g39210-AAL31925, At2g28120-AAL14413, LjN70-AAC3950, OxlT1-Q51330, MCT1-P53986, and GmN70-AY726670.

ACKNOWLEDGMENTS

We thank Dr. Stephen D. Tyerman, Adelaide University, and Dr. C. David Weaver, Vanderbilt University, for constructive comments during the preparation of this manuscript.

Received August 19, 2004; returned for revision October 11, 2004; accepted October 14, 2004.

LITERATURE CITED

Abe K, Ruan ZS, Maloney PC (1996) Cloning, sequencing, and expression in *Escherichia coli* of OxlT, the oxalate:formate exchange protein of *Oxalobacter formigenes*. J Biol Chem **271:** 6789–6793

Arrese-Igor C, Minchin FR, Gordon AJ, Nath AK (1997) Possible causes of physiological decline in soybean nitrogen fixation in the presence of nitrate. J Exp Bot **48:** 905–913

Barbier-Brygoo H, Vinauger M, Colcombet J, Ephritikhine G, Franchisse JM, Maurel C (2000) Anion channels in higher plants: functional characterization, molecular structure and physiological role. Biochim Biophys Acta **1465:** 199–218

Blumwald E, Fortin MG, Rea PA, Verma DPS, Poole RJ (1985) Transport of fixed nitrogen in soybean (*Glycine max*) root nodules. Presence of plasma membrane type H+-ATPase in the peribacteroid membrane. Plant Physiol **78:** 665–672

Brewin NJ (1991) Development of the legume root nodule. Annu Rev Cell Biol **7:** 191–226

Carpenter L, Poole RC, Halestrap AP (1996) Cloning and sequencing of the monocarboxylate transporter from mouse Ehrlich Lettre tumour cell confirms its identity as MCT1 and demonstrates that glycosylation is not required for MCT1 function. Biochim Biophys Acta **1279:** 157–163

Carroll BJ, Hansen AP, McNeil DL, Gresshoff PM (1987) Effect of oxygen supply on nitrogenase activity of nitrate- and dark-stressed soybean (*Glycine max* [L.] Merr.) plants. Aust J Plant Physiol **14:** 679–687

Carroll BJ, Mathews A (1990) Nitrate inhibition of nodulation in legumes. *In* PM Gresshoff, ed, Molecular Biology of Symbiotic Nigrogen Fixation. CRC Press, Boca Raton, FL, pp 159–180

Catalano CM, Lane WS, Sherrier DJ (2004) Biochemical characterization of symbiosome membrane proteins from *Medicago truncatula* root nodules. Electrophoresis **25:** 519–531

Dascal N (1987) The use of Xenopus oocytes for the study of ion channels. CRC Crit Rev Biochem **22:** 317–387

Day DA, Poole PS, Tyerman SD, Rosendahl L (2001) Ammonia and amino acid transport across symbiotic membranes in nitrogen-fixing legume nodules. Cell Mol Life Sci **58:** 61–71

Dean RM, Rivers RL, Zeidel ML, Roberts DM (1999) Purification and functional reconstitution of soybean nodulin 26. An aquaporin with water and glycerol transport properties. Biochemistry **38:** 347–353

Forde BG (2000) Nitrate transporters in plants: structure, function and regulation. Biochim Biophys Acta **1465:** 219–235

Fortin MG, Morrison NA, Verma DP (1987) Nodulin-26, a peribacteroid membrane nodulin is expressed independently of the development of the peribacteroid compartment. Nucleic Acids Res **15:** 813–824

Fortin MG, Zelechowska M, Verma DPS (1985) Specific targeting of membrane nodulins to the bacteroid-enclosing compartment in soybean nodules. EMBO J **4:** 3041–3046

Guenther JF, Chanmanivone N, Galetovic MP, Wallace IS, Cobb JA, Roberts DM (2003) Phosphorylation of soybean nodulin 26 on serine 262 enhances water permeability and is regulated developmentally and by osmotic signals. Plant Cell **15:** 981–991

Guenther JF, Roberts DM (2000) Water-selective and multifunctional aquaporins from *Lotus japonicus* nodules. Planta **210:** 741–748

Jeong J, Suh S, Guan C, Tsay YF, Moran N, Oh CJ, An CS, Demchenko KN, Pawlowski K, Lee Y (2004) A nodule-specific dicarboxylate transporter from alder is a member of the peptide transporter family. Plant Physiol **134:** 969–978

Kaiser BN, Moreau S, Castelli J, Thomson R, Lambert A, Bogliolo S, Puppo A, Day DA (2003) The soybean NRAMP homologue, GmDMT1, is a symbiotic divalent metal transporter capable of ferrous iron transport. Plant J **35:** 295–304

Krieg PA, Melton DA (1984) Functional messenger RNAs are produced by SP6 in vitro transcription of cloned cDNAs. Nucleic Acids Res **12:** 7057–7070

Kyte J, Doolittle RF (1982) A simple method for displaying the hydropathic character of a protein. J Mol Biol **157:** 105–132

Limpens E, Bisseling T (2003) Signaling in symbiosis. Curr Opin Plant Biol **6:** 343–350

Luciński R, Polcyn W, Ratajczak L (2002) Review: nitrate reduction and nitrogen fixation in symbiotic association Rhizobium-legumes. Acta Biochim Pol **49:** 537–546

Machaca K, Hartzell HC (1999) Reversible Ca gradients between the subplasmalemma and cytosol differentially activate Ca-dependent Cl currents. J Gen Physiol **113:** 249–266

Matamoros MA, Baird LM, Escuredo PR, Dalton DA, Minchin FR, Iturbe-Ormaetxe I, Rubio MC, Moran JF, Gordon AJ, Becana M (1999) Stress-induced legume root nodule senescence: physiological, biochemical, and structural alterations. Plant Physiol **121:** 97–112

Moreau S, Thomson RM, Kaiser BN, Trevaskis B, Guerinot ML, Udvardi MK, Puppo A, Day DA (2002) GmZIP1 encodes a symbiosis-specific zinc transporter in soybean. J Biol Chem **277:** 4738–4746

Niemietz CM, Tyerman SD (2000) Channel-mediated permeation of ammonia gas through the peribacteroid membrane of soybean nodules. FEBS Lett **465:** 110–114

Orsel M, Filleur S, Fraisier V, Daniel-Vedele F (2002) Nitrate transport in plants: which gene and which control? J Exp Bot **53:** 825–833

Ou Yang LJ, Udvardi MK, Day DA (1990) Specificity and regulation of the

dicarboxylate carrier on the peribacteroid membrane of soybean nodules. Planta **182:** 437–444

Panter S, Thomson R, de Bruxelles G, Laver D, Trevaskis B, Udvardi MK (2000) Identification with proteomics of novel proteins associated with the peribacteroid membrane of soybean root nodules. Mol Plant Microbe Interact **13:** 325–333

Pao SS, Paulsen IT, Saier MH Jr (1998) Major facilitator superfamily. Microbiol Mol Biol Rev **62:** 1–34

Preston GM, Carroll TP, Guggino WB, Agre P (1992) Appearance of water channels in Xenopus oocytes expressing red cell CHIP28 protein. Science **256:** 385–387

Rivers RL, Dean RM, Chandy C, Hall JE, Roberts DM, Zeidel ML (1997) Functional analysis of nodulin 26, an aquaporin in soybean root nodule symbiosomes. J Biol Chem **272:** 16256–16261

Roberts DM, Tyerman SD (2002) Voltage-dependent cation channels permeable to NH(+)(4), K(+), and Ca(2+) in the symbiosome membrane of the model legume *Lotus japonicus*. Plant Physiol **128:** 370–378

Roth E, Jeon K, Stacey G (1988) Homology in endosymbiotic systems: the term 'symbiosome.' *In* R Palcios, DPS Verma, eds, Molecular Genetics of Plant Microbe Interactions. ADS Press, St. Paul, pp 220–225

Saalbach G, Erik P, Wienkoop S (2002) Characterisation by proteomics of peribacteroid space and peribacteroid membrane preparations from pea (*Pisum sativum*) symbiosomes. Proteomics **2:** 325–337

Sambrook J, Fritsch EF, Maniatis T (1989) Molecular Cloning: A Laboratory Manual, Ed 2. Cold Spring Harbor Laboratory Press, Cold Spring Harbor, NY

Stougaard J (2000) Regulators and regulation of legume root nodule development. Plant Physiol **124:** 531–540

Streeter JG (1988) Inhibition of legume nodule formation and N_2 fixation by nitrate. CRC Crit Rev Plant Sci **7:** 1–23

Szczyglowski K, Kapranov P, Hamburger D, de Bruijn FJ (1998) The *Lotus japonicus* LjNOD70 nodulin gene encodes a protein with similarities to transporters. Plant Mol Biol **37:** 651–661

Tyerman SD, Whitehead LF, Day DA (1995) A channel-like transporter for NH4+ on the symbiotic interface of N2-fixing plants. Nature **378:** 629–632

Udvardi MK, Day DA (1989) Electrogenic ATPase activity on the peribacteroid membrane of soybean (*Glycine max* L.) root nodules. Plant Physiol **90:** 982–987

Udvardi MK, Day DA (1997) Metabolite transport across symbiotic membranes of legume nodules. Annu Rev Plant Physiol Plant Mol Biol **48:** 493–523

Udvardi MK, Lister DL, Day DA (1991) ATPase activity and anion transport across the peribacteroid membrane of isolated soybean symbiosomes. Arch Microbiol **156:** 362–366

Weaver CD, Crombie B, Stacy G, Roberts DM (1991) Calcium-dependent phosphorylation of symbiosome membrane proteins from nitrogen-fixing soybean nodules: evidence for phosphorylation of nodulin 26. Plant Physiol **95:** 222–227

Wienkoop S, Saalbach G (2003) Proteome analysis. Novel proteins identified at the peribacteroid membrane from *Lotus japonicus* root nodules. Plant Physiol **131:** 1080–1090

Zhang Y, Roberts DM (1995) Expression of soybean nodulin 26 in transgenic tobacco. Targeting to the vacuolar membrane and effects on floral and seed development. Mol Biol Cell **6:** 109–117